



PREPARATION OF Gd₂O₃ NANOMATERIALS VIA SOLUTION COMBUSTION SYNTHESIS FOR OXIDATIVE COUPLING OF METHANE

Hasan ÖZDEMİR^{1,*}

¹ Chemical Engineering Department, Engineering Faculty, İstanbul University-Cerrahpasa, İstanbul, Turkey

ABSTRACT

In this study, in the production of Gd₂O₃ material which has many usage areas, solution combustion synthesis was used and the changes in the physical and structural properties of the material were investigated by changing the oxidant/fuel ratio. The resulting metal oxide powders were characterized by X-ray diffraction (XRD), Brunauer-Emmett-Teller (BET) surface area, Thermogravimetric-Differential thermal analysis (TG-DTA) and scanning electron microscopy (SEM) analysis and tested in oxidative coupling of methane. Cubic and monoclinic phases were observed in Gd₂O₃ crystal structure at fuel-rich and stoichiometric conditions, and only cubic phase was determined at fuel-lean conditions. It was determined that the obtained powders were mesoporous and the highest BET surface area was obtained at stoichiometric oxidant/fuel ratio (18.6 m²/g). It was determined that the powders were formed from rather small particles (<35 nm) and with layered or stacked structure. The catalytic performance of Gd₂O₃ nanoparticles was found to be dependent on the BET surface area and crystal structure. The highest C₂ yield (8.5%) was obtained at 720°C with the Gd₂O₃ that was synthesized using the equivalence ratio of 0.5.

Keywords: Gd₂O₃, Solution combustion synthesis, Oxidative coupling of methane

1. INTRODUCTION

Gadolinium oxide (Gd₂O₃) is a rare earth metal oxide that can be used in many areas such as magnetic storage, microwave absorption, catalysis, cell separation, magnetic resonance imaging, tissue repair and drug release, and studies are underway to synthesize with appropriate properties according to the area of use [1]. Gd₂O₃ is generally used as a support structure or as an additive in addition to its use as a catalyst in oxidation reactions due to its high thermal resistance and high surface alkalinity. For these reasons, it is important that the gadolinium oxide to be used as support must have a high surface area and high crystallinity.

In literature, various methods such as sol-gel [2], solution combustion [3], polyol [4], flame pyrolysis [5], hydrothermal [6] synthesis methods were used for the synthesis of Gd₂O₃. Amongst these, solution combustion synthesis is a very practical and low-cost method due to low energy consumption, high purity product formation and time efficiency [7]. The method is simply based on the exothermic reaction of the gaseous products released as a result of the rapid heating the aqueous solution of metal nitrate salts and of the fuel so that the temperature is elevated to allow the desired product to be obtained.

Oxidative coupling of methane (OCM), which produces ethane and ethylene from methane directly, is a very promising and attractive reaction for both academia and industry. This reaction involves both methane and oxygen reacting to yield ethane and ethylene generally at high reaction temperatures (600-900°C) on a catalyst [8, 9]. Na₂WO₄/Mn/SiO₂ and Li/MgO catalysts were the most investigated catalysts in the literature and showed high performance at high temperatures (>750°C). However, it was found that the rare earth metal oxides (La₂O₃, Sm₂O₃, etc.) showed higher activity and selectivity than these catalysts at lower temperatures (<700°C) for the OCM reaction [10–12]. Although there are many articles about the catalytic performance of La₂O₃ and Sm₂O₃ in the literature, the performance of Gd₂O₃ was not investigated especially at lower temperatures (<700°C)

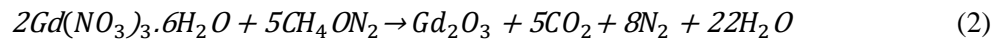
*Corresponding Author: hasan.ozdemir@istanbul.edu.tr
Received:27.06.2019 Published: 31. 03.2020

Considering the above-mentioned issues, solution combustion synthesis was used for the direct preparation of Gd₂O₃ which can be used as catalyst or support material and the effect of oxidant/fuel ratio on the material structure and physicochemical properties were investigated in this work. The effect of oxidant/fuel ratio on the catalytic performance of the materials was evaluated in the oxidative coupling of methane between 450-750°C.

2. MATERIALS AND METHODS

For the preparation of Gd₂O₃ by the solution combustion synthesis, the stoichiometric oxidant/fuel ratio of the structure was determined by using Equation 1, and the amounts of salt and urea were calculated so that the amount of fuel (urea) to be used was 0.5, 1 and 2 times of the stoichiometric ratio. The stoichiometric ratio was found to be 5/2 as given in Equation 2 and thus, the amount of stoichiometric urea (Sigma Aldrich -> 99.5%) was calculated as 2.5 moles per one mole of Gd(NO₃)₃.6H₂O (Sigma Aldrich-99.9%). The equivalence ratio (ϕ_e) of 0.5 (fuel-rich) and 2 (fuel-lean) mean 2 and 0.5 times the amount of the stoichiometric amount of urea. For each synthesis, 25 ml of water-dissolved salt and urea mixture was treated in a pre-heated oven at 500°C for 2 hours. No further heat treatment was applied during the treatment. The obtained powders were named according to the used equivalence ratio for the synthesis as the “Gd₂O₃-equivalence ratio”.

$$\phi_e = \frac{\text{Valencies of all oxidizing and reducing elements in oxidizer}}{(-1) \sum \text{Valencies of all oxidizing and reducing elements in fuel}} = \frac{p}{r} \quad (1)$$



The thermal behaviors of each sample solution and obtained powders were investigated with the SEIKO II Exstar TG/DTA 6300 device. The analyzes were carried out between 30-950°C with 20°C/min increment under synthetic air flow of 50 ml/min.

Crystal structures of the obtained samples were determined by XRD analysis. The analyzes were carried out with a Rigaku D/Max-2200 XRD apparatus between 10-90° under Cu/K α ray with 1.54 Å wavelength. The Scherrer equation (3) was used to calculate the mean crystallite size.

$$d = \frac{0,9 \times \lambda_{K\alpha Cu}}{B_{2\theta} \times \text{Cos}\theta_{max}} \quad (3)$$

- d : Mean crystallite size (Å)
- $\lambda_{K\alpha Cu}$: X-ray wavelength (1,54056 Å)
- θ_{max} : Scattering angle of maximum intensity peak (Rad)
- $B_{2\theta}$: Full width at half maximum intensity of the peak (Rad)

BET surface areas and pore-diameter distributions of the obtained structures were performed with Quantachrome Nova 3200e Model automatic surface area and pore size analyzer. N₂ gas was used as the adsorbate and the analyzes were carried out at -196 ° C with liquid nitrogen between 0-1 relative partial pressure range using 40 different adsorption and 24 different desorption points. Prior to analysis, the samples were dried for 3 hours at 300°C under vacuum. The BET surface area and pore-diameter distribution results were determined by the software of the device.

The morphology of the samples were revealed with QUANTA FEG 450 (FEI) SEM equipment after coating with Au/Pd alloy. The images were taken under high vacuum and at 30 kV.

The catalytic performances of the samples for oxidative coupling of methane (OCM) were evaluated with Microreactor (Hiden Analytical)-GC (Agilent 7890A). Prior to the analysis, 100 mg catalyst sample was flushed with 60 ml/min N₂ flow from room temperature to 450°C. The tests were conducted with the ratio of CH₄/O₂/N₂: 42/14/4 under 36,000 l kg⁻¹ h⁻¹ from 450°C to 750°C with 30°C intervals. The carbon balances were always within 100%±5. The details about the configuration and calculations could be found elsewhere.

3. RESULTS AND DISCUSSION

TG/DTA analyzes were performed to investigate the thermal behavior of urea/metal salt mixtures prepared prior to the synthesis of Gd₂O₃ support structures. In this way, it was determined at which temperature the mixtures should be burned without leaving any residue.

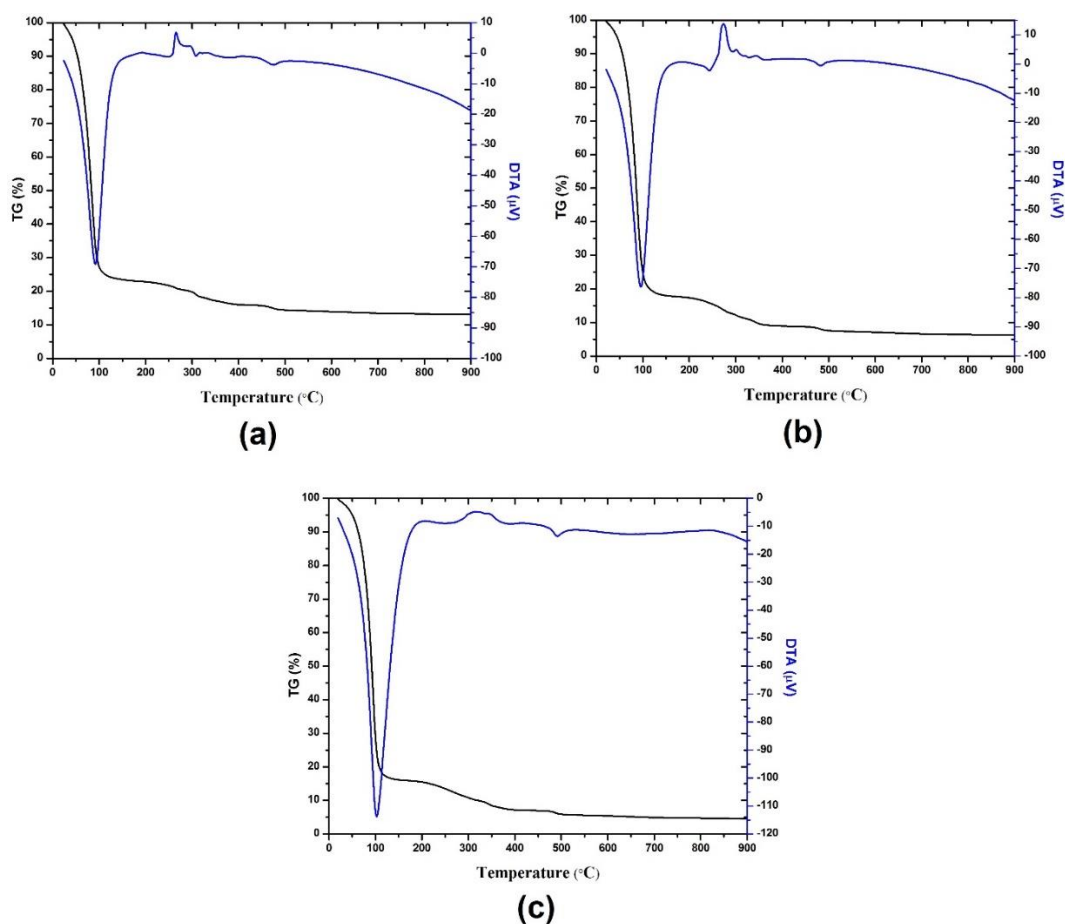


Figure 1. TG/DTA results of Gd₂O₃ synthesis solutions a) Gd₂O₃-2 b) Gd₂O₃-1 c) Gd₂O₃-0,5

The TG/DTA results of the Gd₂O₃ synthesis solutions were given in Figure 1. Similar thermal behavior was observed for each ratio. The intense endothermic peak at 100°C was due to the water evaporation, while the endothermic peak at 243°C was due to the loss of crystal water and nitrate decomposition. It was thought that the exothermic peaks observed between 275-343°C occurred as a result of combustion and the endothermic peak at 481°C, which was observed with a weight loss of 1.5%, belonged to decarbonization and dehydroxylation. According to TG/DTA results, the lowest burning temperature was determined as 500°C without leaving any residues. In the TG/DTA analysis of the powders obtained after the synthesis, the weight loss with the decreasing equivalence ratio was determined as 4%, 7% and 4%, respectively possibly due to the desorption of adsorbates like moisture and CO₂.

XRD spectra of the samples for the determination of the crystal structures of the materials obtained were given in Figure 2. It was observed that cubic (JCPDS 43-1014) and monoclinic (JCPDS 43-1015) Gd_2O_3 formed when the equivalence ratio was 0.5. The main phase was cubic and very low amounts of monoclinic phase was determined in the case of Gd_2O_3 -1. Only the cubic Gd_2O_3 phase was observed for Gd_2O_3 -2. Similarly, in a study using only an equivalence ratio of 0.5, and combustion at 300°C, the structure of Gd_2O_3 was found to contain cubic and monoclinic phases [13]. In another study with an equivalence ratio of 1 and combustion at 300°C, Gd_2O_3 was found to be amorphous and subjected to calcination at 800°C [14]. These results revealed that the oxidant/fuel ratio and the processing temperature are the most important parameters in the direct production of metal oxide materials by the solution combustion synthesis. The results obtained in this work showed that the production of well-crystallized Gd_2O_3 was possible even at low amounts of urea use by using appropriate combustion temperature. When the crystallite sizes of the structures were examined (Table 1), it was determined that the crystallite sizes increased with the decreasing equivalence ratio. The decrease in equivalence ratio means an increase in fuel amount, more heat was released during combustion and led to the sintering of structures.

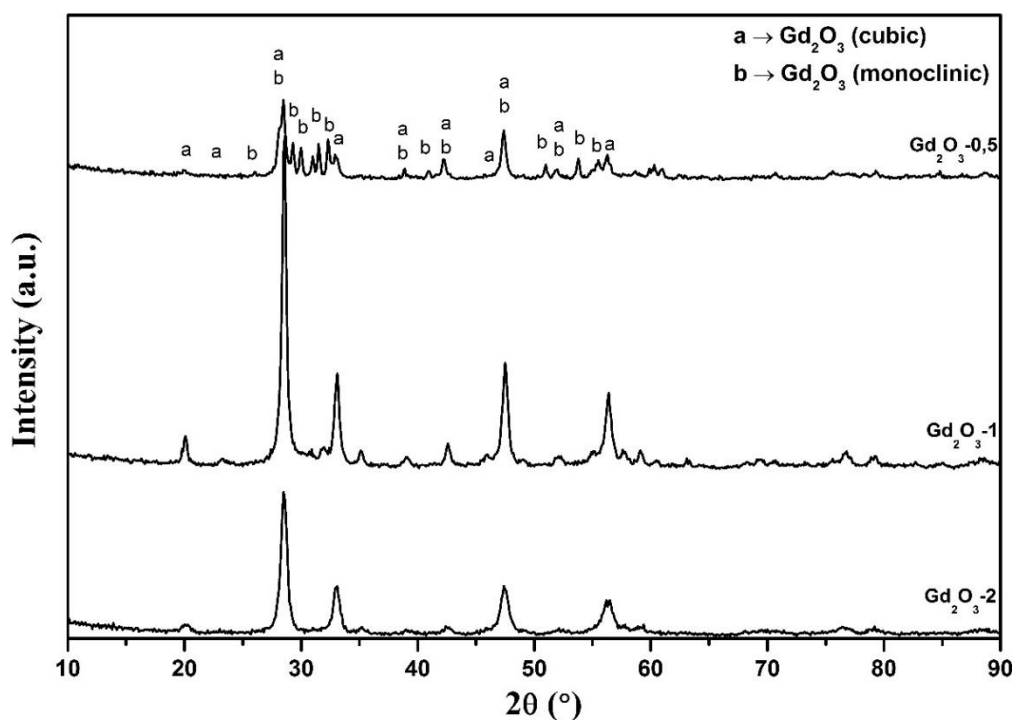


Figure 2. XRD spectra of Gd_2O_3 samples

Table 1. BET surface area, total pore volume and mean pore size of Gd_2O_3 samples

Sample	Crystallite Size (nm)	BET surface area (m^2/g)	Total pore volume (ml/g)	Mean pore size (nm)
Gd_2O_3 -0,5	20.5 (31,7 ¹)	12.6	0.07	5.9
Gd_2O_3 -1	18.8	18.6	0.083	6.7
Gd_2O_3 -2	13.4	5.9	0.019	3.9

¹ Monoclinic phase

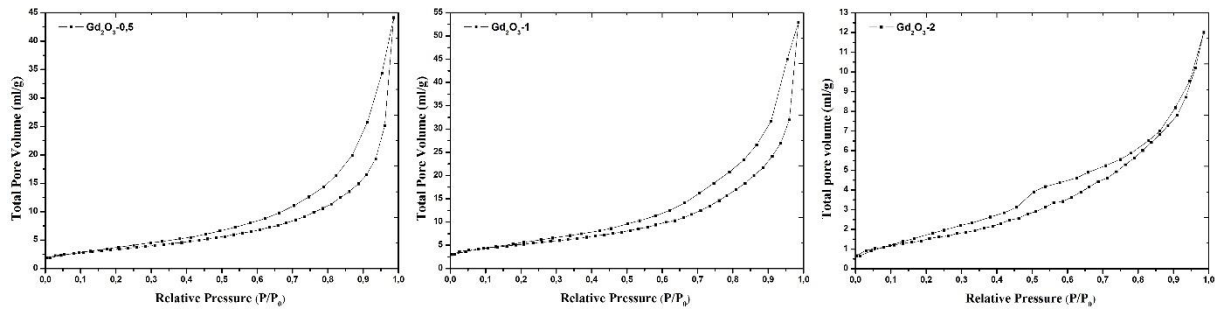


Figure 3. N₂ adsorption-desorption isotherms of Gd₂O₃ samples

The N₂ adsorption-desorption isotherms of the Gd₂O₃ samples were given in Figure 3, while the BET surface area, pore volume and mean pore size results were given in Table 1. The isotherms obtained were Type 4 according to the IUPAC classification generally obtained for mesoporous (5-50 nm) structures [15]. The BET surface area results showed that the surface area increased with an increasing equivalence ratio and then decreased by almost 3 times. The pore volume and pore diameter showed a similar trend. The highest BET surface area was obtained when the equality ratio was 1 (18.6 m²/g). The reduction of BET surface area in Gd₂O₃-0.5 was thought to be due to the phase change.

SEM images of the samples were given in Figure 4. It was observed that the structure Gd₂O₃-2 formed in superimposed layers (Figure 4a) and these structures composed of small (<35 nm) crystals. For Gd₂O₃-1 (Figure 4b), it could be seen that the macro-pores formed and the layers become more pronounced. Macro-pores were still evident on Gd₂O₃-0.5 (Figure 4c), but the structure composed of nanoparticle stacks.

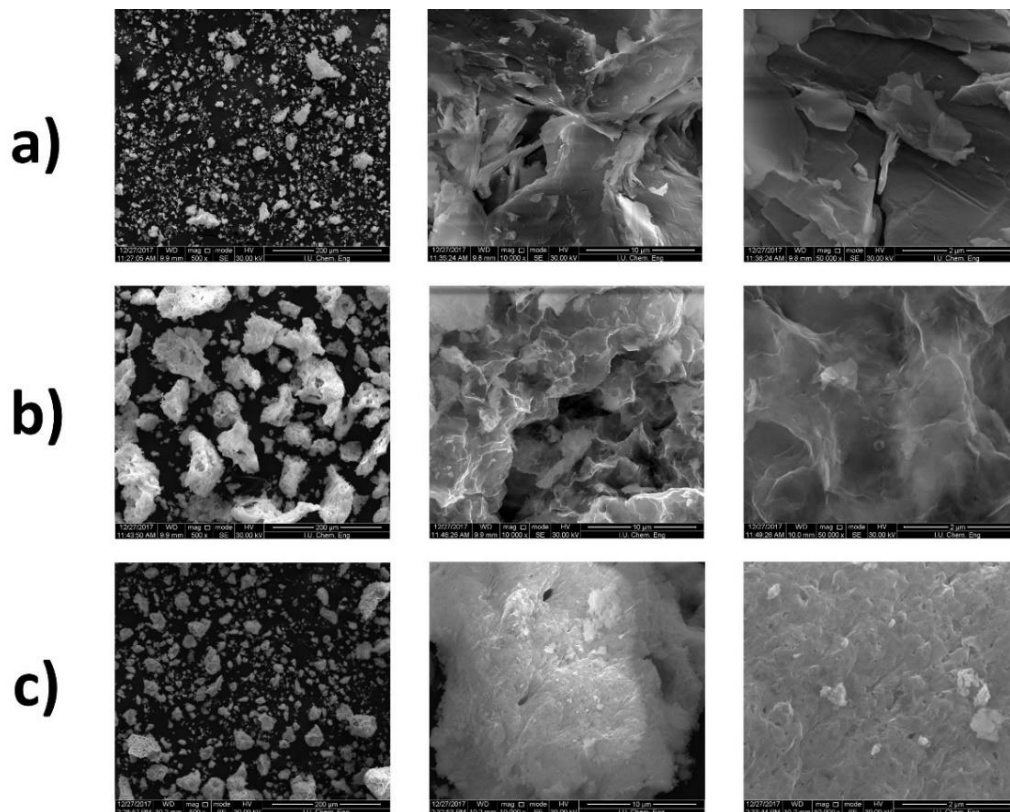


Figure 4. SEM images of Gd₂O₃ samples a) Gd₂O₃-2 b) Gd₂O₃-1 c) Gd₂O₃-0,5

The catalytic performances of Gd_2O_3 samples in oxidative coupling of methane between 450-750°C were given in Figure 5. Methane conversion was very low (<3%) at 450°C and 480°C for $Gd_2O_3-0.5$ and Gd_2O_3-1 . However, the coupling reaction took place at 510°C and the methane conversion and C_2 selectivity increased greatly at this temperature. The reaction initiated at 540°C for Gd_2O_3-2 . The methane conversion and C_2 selectivity increased with increasing temperature for all samples. The methane conversion, C_2 selectivity, C_2H_4/C_2H_6 ratio and C_2 yield were found always higher than the other samples at all temperatures for $Gd_2O_3-0.5$. While the methane conversions were close for Gd_2O_3-1 and Gd_2O_3-2 , C_2 selectivity of Gd_2O_3-2 was higher than Gd_2O_3-1 between 540-750°C. Similar trends were observed for C_2H_4/C_2H_6 ratio and C_2 yield. No correlation could be found between crystallite size and catalytic activity or selectivity. However, in the literature, it was shown that the increase in BET surface area of Li/MgO catalyst decreases the C_2 selectivity [16]. In this work the BET surface area of Gd_2O_3-1 was higher than that of Gd_2O_3-2 and the crystal structure of these materials were mainly cubic Gd_2O_3 . Thus, it could be concluded that the higher C_2 selectivity of Gd_2O_3-2 compared to Gd_2O_3-1 was mainly due to the lower BET surface area of Gd_2O_3-2 . However, the C_2 selectivity results obtained with $Gd_2O_3-0.5$ suggested that the BET surface area was not the only parameter affected the selectivity of the Gd_2O_3 catalysts because the surface area of Gd_2O_3-1 was higher than that of Gd_2O_3-2 . Thus, the higher performance of Gd_2O_3-2 was attributed to the presence of both cubic and monoclinic crystal structures in the sample. Similar results were observed for Sm_2O_3 catalysts in the literature which supported the obtained conclusion [17]. Additionally, the presence of two phase seem to be beneficial for the dehydrogenation of C_2H_6 as could be seen from the results. It is interesting to note that, the bulk density of the materials followed the order of $Gd_2O_3-1 < Gd_2O_3-2 < Gd_2O_3-0.5$ which was similar to the C_2 selectivity order. Therefore, it could be said that the catalyst bed length might also have an effect on C_2 selectivity. Because, the shorter the length of the bed, the C_2 products reaches the exit quicker, and decreasing the possibility of transformation into CO_x products.

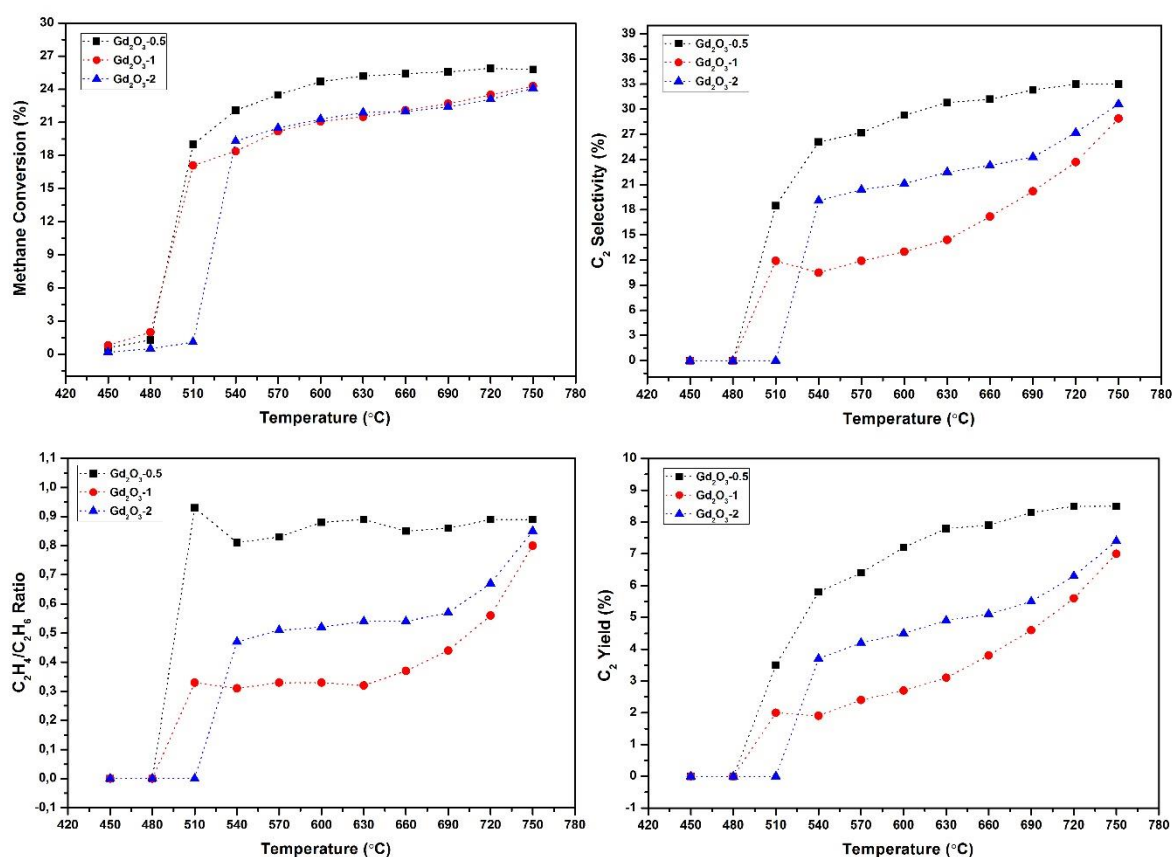


Figure 5. OCM performances of Gd_2O_3 samples

It is not appropriate to directly compare the catalyst performances with different works due to the usage of different reaction conditions. However, $Gd_2O_3-0.5$ showed the highest C_2 yield (8.5%) at $720^\circ C$, which is higher than many rare earth oxide catalysts (like Sm_2O_3 and Gd_2O_3) [18–21]. Additionally, the C_2 yield was higher than the well-known $4Li/MgO$ but lower than $2Mn/5Na_2WO_4/SiO_2$ and La_2O_3 catalysts at close reaction conditions [19, 22].

4. CONCLUSIONS

In this work Gd_2O_3 materials were synthesized via solution combustion synthesis method and the effect of oxidant/fuel ratio on the structure and catalytic performance for OCM reaction was investigated. It was observed that it was possible to obtain well crystallized Gd_2O_3 metal oxide structures by using appropriate oxidant/fuel ratio and ignition temperature. The obtained phases were cubic and monoclinic when the equivalence ratio decreased to the ratio of 2. The main phase was cubic for the equivalence ratio of 0.5 and 1. All of the materials synthesized were mesoporous. SEM images showed that the materials composed of layers or stacks. The catalytic performance of Gd_2O_3 nanoparticles were found to be dependent on the BET surface area and crystal structure. The catalyst bed length might also have an effect on C_2 selectivity. Although lower BET surface area enhanced the C_2 selectivity, the presence of both cubic and monoclinic phases greatly increased the C_2 selectivity and yield of the Gd_2O_3 catalyst. The highest C_2 yield was obtained at $720^\circ C$ with $Gd_2O_3-0.5$ (8.5%).

ACKNOWLEDGEMENTS

This study was supported by Istanbul University-Cerrahpaşa Research Fund through project no: 24133.

REFERENCES

- [1] Ahab A, Rohman F, Iskandar F, Haryanto F, Arif I. A simple straightforward thermal decomposition synthesis of PEG-covered Gd_2O_3 ($Gd_2O_3@PEG$) nanoparticles. *Adv Powder Technol* 2016; 27: 1800–1805.
- [2] Lin C-C, Lin K-M, Li Y-Y. Sol–gel synthesis and photoluminescent characteristics of Eu^{3+} -doped Gd_2O_3 nanophosphors. *J Lumin* 2007; 126: 795–799.
- [3] Dhananjaya N, Nagabhushana H, Nagabhushana BM, Chakradhar RP., Shivakumara C, Rudraswamy B. Synthesis, characterization and photoluminescence properties of $Gd_2O_3:Eu^{3+}$ nanophosphors prepared by solution combustion method. *Phys B Condens Matter* 2010; 405: 3795–3799.
- [4] Müller A, Heim O, Panneerselvam M, Willert-Porada M. Polyol method for the preparation of nanosized Gd_2O_3 , boehmite and other oxides. *Mater Res Bull* 2005; 40: 2153–2169.
- [5] Goldys EM, Drozdowicz-Tomsia K, Jinjun S, Dosev D, Kennedy IM, Yatsunencko S, et al. Optical Characterization of Eu-Doped and Undoped Gd_2O_3 Nanoparticles Synthesized by the Hydrogen Flame Pyrolysis Method. *J Am Chem Soc* 2006; 128: 14498–14505.
- [6] Liu G, Hong G, Wang J, Dong X. Hydrothermal synthesis of spherical and hollow $Gd_2O_3:Eu^{3+}$ phosphors. *J Alloys Compd* 2007; 432: 200–204.
- [7] Wen W, Wu J-M. Nanomaterials via solution combustion synthesis: a step nearer to controllability. *RSC Adv* 2014; 4: 58090–58100.

- [8] Galadima A, Muraza O. Revisiting the oxidative coupling of methane to ethylene in the golden period of shale gas: A review. *J Ind Eng Chem* 2016; 37: 1-13.
- [9] Farrell BL, Igenegbai VO, Linic S. A Viewpoint on Direct Methane Conversion to Ethane and Ethylene Using Oxidative Coupling on Solid Catalysts. *ACS Catal* 2016; 6-7: 4340-4346.
- [10] Karakaya C, Kee RJ. Progress in the direct catalytic conversion of methane to fuels and chemicals. *Prog Energy Combust Sci* 2016; 55: 60-97.
- [11] Alexiadis VI, Chaar M, van Veen A, Muhler M, Thybaut JW, Marin GB. Quantitative screening of an extended oxidative coupling of methane catalyst library. *Appl Catal B Environ* 2016; 199: 252-259.
- [12] Jiang T, Song J, Huo M, Yang NT, Liu J, Zhang J, et al. La_2O_3 catalysts with diverse spatial dimensionality for oxidative coupling of methane to produce ethylene and ethane. *RSC Adv* 2016; 6: 34872–34876.
- [13] Tamrakar RK, Bisen DP, Brahme N. Comparison of photoluminescence properties of Gd_2O_3 phosphor synthesized by combustion and solid state reaction method. *J Radiat Res Appl Sci* 2014; 7: 550–559.
- [14] Dhananjaya N, Nagabhushana H, Nagabhushana BM, Rudraswamy B, Sharma SC, Sunitha DV, et al. Effect of different fuels on structural, thermo and photoluminescent properties of Gd_2O_3 nanoparticles. *Spectrochim Acta Part A Mol Biomol Spectrosc* 2012; 96: 532–540.
- [15] Sing KSW. Reporting physisorption data for gas/solid systems with special reference to the determination of surface area and porosity (Recommendations 1984). *Pure Appl Chem* 1985; 57: 603–619.
- [16] Kuo Y, Behrendt F, Lerch M. Effect of the Specific Surface Area of Li/MgO Catalysts in the Oxidative Coupling of Methane. *Zeitschrift Für Phys Chemie* 2007; 221: 1017–1037.
- [17] Korf SJ, Roos JA, Diphoorn JM, Veehof RHJ, van Ommen JG, Ross JRH. The selective oxidation of methane to ethane and ethylene over doped and un-doped rare earth oxides. *Catal Today* 1989; 4: 279–292.
- [18] Au CT, Chen KD, Ng CF. The modification of Gd_2O_3 with BaO for the oxidative coupling of methane reactions. *Appl Catal A Gen* 1998; 170: 81–92.
- [19] Özdemir H, Öksüzömer MAF, Ali Gürkaynak M. Studies on oxidative coupling of methane using Sm_2O_3 -based catalysts. *Chem Eng Commun* 2019; 206: 48–60.
- [20] Papa F, Luminita P, Osiceanu P, Birjega R, Akane M, Balint I. Acid–base properties of the active sites responsible for C_2^+ and CO_2 formation over $\text{MO-Sm}_2\text{O}_3$ ($\text{M} = \text{Zn, Mg, Ca}$ and Sr) mixed oxides in OCM reaction. *J Mol Catal A Chem* 2011; 346: 46–54.
- [21] Elkins TW, Hagelin-Weaver HE. Oxidative coupling of methane over unsupported and alumina-supported samaria catalysts. *Appl Catal A Gen* 2013; 454: 100–114.
- [22] Huang P, Zhao Y, Zhang J, Zhu Y, Sun Y. Exploiting shape effects of La_2O_3 nanocatalysts for oxidative coupling of methane reaction. *Nanoscale* 2013; 5: 10844–10848.